

Spatio-Temporal State Space Model For Efficient Event-Based Optical Flow

Muhammad Ahmed Humais¹ Xiaoqian Huang¹ Hussain Sajwani¹ Sajid Javed² Yahya Zweiri¹
¹Advanced Research and Innovation Center (ARIC), Khalifa University, Abu Dhabi, UAE
²Department of Computer Science, Khalifa University of Science and Technology, Abu Dhabi, UAE

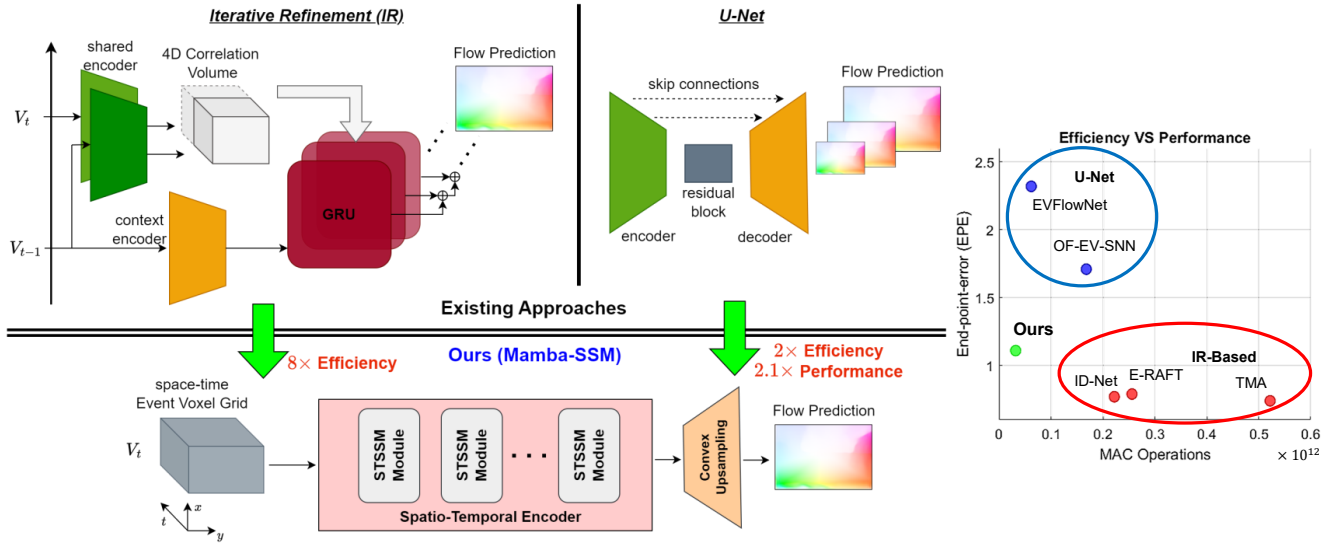


Figure 1. **Top-Left** Previous work used either computationally expensive iterative refinement (IR) framework [10, 20] or U-Net architecture with suboptimal performance. **Bottom-Left** we solved this issue with a novel network architecture (Sec. 3.2) that leverages our cutting-edge Spatio-Temporal State Space Model (STSSM) module (Sec. 3.3) for highly efficient spatio-temporal feature extraction and convex upsampling to predict full resolution optical flow with less computations compared to a decoder. **Right** Comparison of existing approaches in terms of computational efficiency and performance on DSEC public benchmark [9].

Abstract

Event cameras unlock new frontiers that were previously unthinkable with standard frame-based cameras. One notable example is low-latency motion estimation (optical flow), which is critical for many real-time applications. In such applications, the computational efficiency of algorithms is paramount. Although recent deep learning paradigms such as CNN, RNN, or ViT have shown remarkable performance, they often lack the desired computational efficiency. Conversely, asynchronous event-based methods including SNNs and GNNs are computationally efficient; however, these approaches fail to capture sufficient spatio-temporal information, a powerful feature required to achieve better performance for optical flow estimation. In this work, we introduce Spatio-Temporal State Space Model (STSSM) module along

with a novel network architecture to develop an extremely efficient solution with competitive performance. Our STSSM module leverages state-space models to effectively capture spatio-temporal correlations in event data, offering higher performance with lower complexity compared to ViT, CNN-based architectures in similar settings. Our model achieves $4.5\times$ faster inference and $8\times$ lower computations compared to TMA and $2\times$ lower computations compared to EV-FlowNet with competitive performance on the DSEC benchmark. Our code will be available at <https://github.com/AhmedHumais/E-STMFlow>.

1. Introduction

Optical flow is a fundamental computer vision problem with numerous practical applications. From frame-based camera perspective, optical flow is estimated between two consec-

utive frames, hence the maximum update rate is limited by the frame rate of the camera. Due to microsecond temporal resolution, event cameras offer unique advantages, allowing for high update rate and high-bandwidth optical flow estimation [11, 24].

In contrast to frame-based cameras that encode spatial and color information at a fixed frame rate. Event cameras encode spatio-temporal motion information of edges. Currently, most state-of-the-art approaches obtain frame-like representation of event data [10, 11, 17, 19, 20, 24, 31, 36, 37] to use CNNs or RNNs which incur huge computational overhead. To address this, sparse and asynchronous computational paradigms have been explored such as Spiking Neural Networks (SNNs) [2, 25] and Graph Neural Networks (GNNs) [3]. Although such methods significantly drop the computational overhead, however, the performance they offer is not comparable to state-of-the-art CNN, RNN [10, 20, 34] and ViT-based [19, 31] methods. In this work, we focus on developing a light-weight solution for event-based optical flow by leveraging state-space models (SSMs) that are better suited for spatio-temporal event data.

In terms of network architecture, existing methods for event-based optical flow can be broadly categorized into two types. The first type includes methods that draw inspiration from U-Net architecture [23, 36], and sometimes involve SNNs [2, 15, 17, 25], RNNs [4, 15, 24] or ViT [31, 35]. The other type includes the methods that employ some kind of iterative refinement (IR) inside the network using a recurrent unit such as GRU [10, 11, 19, 20, 22, 34]. IR can be viewed as an optimization framework embedded into a neural network. While effective, this approach typically incurs computational cost that is several times higher than that of U-Net-like architectures [10, 34, 36]. We depart from traditional network architectures to introduce a novel design that does not rely on multiple iterations, contextual information, or prior flow estimates. Our network delivers competitive performance compared to IR-based designs and outperforms U-Net-like architectures.

Due to microsecond temporal resolution, event cameras offer unparalleled edge in highly dynamic scenes. However, in such scenarios, high throughput of the sensor data needs efficient and fast processing algorithms. With linear scaling in sequence length, structured state space models (SSMs) [12, 14, 28] promise huge potential for such rich spatio-temporal event data. SSMs, originally used to model linear time-invariant (LTI) systems, have proven effective in modeling long-range dependencies (LRDs) in a highly efficient manner compared to existing SOTA methods such as CNN, RNN and Transformers. We argue that SSMs, due to their ability of modeling system dynamics, are inherently suitable for processing such kind of dynamic signal with temporal consistency. Our findings support the above argument, as we show that SSMs boast superior per-

formance with much less computations compared to vanilla transformer within the same network architecture.

In this work, we present a novel **Spatio-Temporal SSM** (STSSM) module to address the unique spatio-temporal nature of input event data. Inspired by RAFT [30], we introduced convex upsampling for dense optical flow prediction at full-scale resolution. This allows to significantly reduce the computational cost compared to U-Net architecture, where a decoder with skip connections is used for the same purpose. Finally, we share important insights from our findings about structured SSMs such as S4 [14], S4D [13] and S5 [28] that model LTI systems compared to Mamba [12], which models linear time-variant (LTV) system. Our results show competitive performance compared to SOTA methods on public DSEC [9] dataset.

Our main contributions are summarized below:

- We propose a novel network architecture, different from existing U-Net-based or IR-based networks, our model introduces a spatio-temporal encoder for event volumes and uses efficient convex upsampling for full-scale dense flow prediction.
- We developed a novel STSSM module to leverage SSMs for extracting spatial and temporal dynamics of the scene, encoded in event data and demonstrate its effectiveness compared to ViT.
- Our experimental results demonstrate a substantial reduction in computational cost while maintaining competitive performance relative to state-of-the-art methods. Additionally, our findings offer valuable insights into the use of SSMs for efficient processing of spatio-temporal data.

2. Related Work

Optical flow estimation has been the subject of extensive research for frame-based cameras with numerous notable contributions over the years. However, in this section we will limit our discussion to event-based flow approaches and the recent advancements in SSMs for vision tasks.

2.1. Event-Based Optical Flow

Event-based optical flow approaches can be broadly classified into two major paradigms. Optimization-based approaches and learning-based approached. Optimization-based approaches mostly build on *contrast maximization* with the idea of finding spatio-temporal warping of events that generate the sharpest image [7, 24, 27, 29]. The same idea is applied in various self-supervised learning-based approaches for training the deep neural networks [15, 36, 37].

In terms of network design, the learning-based approaches can be classified into two major paradigms. In fact, these paradigms are borrowed from frame-based optical flow approaches; FlowNet [5] and RAFT [30]. FlowNet proposed a U-Net architecture to predict optical flow from successive frames, which was adapted by EV-FlowNet [36]

for events by obtaining a frame-like representation. Later several works were based on the similar architecture with slight modifications [2, 15–17, 24, 37]. While effective for small pixel displacement, the U-Net architecture struggles when flow magnitude is high. E-RAFT [10], the event-based version of RAFT [30] solved this issue by incorporating iterative-refinement (IR) framework. Their approach involves using successive event volumes to build a spatial pyramid of 4D correlation volumes (CVs). However, processing full 4D correlation volume is prohibitively expensive, hence iterative refinement guides the *lookup* to extract local spatio-temporal correlations from full 4D CVs. Several state-of-the-art methods [11, 19, 20, 22, 33] build on similar principle as it somehow embeds optimization into the network and offer huge performance advantage over U-Net. Nevertheless, IR-based approaches are computationally very expensive, hence the need for efficient high-performance flow estimation method remains an open problem.

Another line of research, investigated light-weight spiking neural networks (SNNs) and graph neural network (GNNs) [1–3, 15–17]. Though computationally efficient, they fail to provide comparative performance to SOTA IR-based methods.

2.2. Vision State Space Models

Structured state space models (SSMs) have rapidly evolved into promising alternative to existing CNN, RNN and Transformer-based methods [12–14, 28]. They offer linear scaling of computational complexity with sequence length and state-of-the-art performance in finding long-range dependencies (LRDs). Recently, their application in vision tasks has been studied [21, 38] as well as for video understanding [18]. From event-based vision perspective, Zubic et al. combined SSMs with attention mechanism for event-based object detection task [39]. However, purely SSM-based approaches for event vision holds huge potential [26].

In our study, for the first time we study the use of SSMs for spatio-temporal data. The space-time coordinates of events are discretized to create spatio-temporal voxel grid, where the discretization error and the polarity is encoded [37]. We reveal that SSMs can efficiently handle such data and provide advantage over vanilla transformers in this specific scenario.

3. Methods

In this section, firstly we present optical flow problem from brightness constancy and spatial consistency constraints to establish the need for spatio-temporal correlations. Then we relate the optical flow problem to event generation model of the event camera and introduce state-space models for optical flow (Sec.3.1). The above discussion sets the stage

for our novel network design (Sec.3.2) and STSSM block (Sec.3.3).

3.1. Preliminaries

3.1.1 Optical Flow

Optical flow estimation relies on the brightness constancy (BC) assumptions. Consider $\mathbf{u} \doteq (u, v)^T$ being pixel coordinate and $I(\mathbf{u}, t)$ being the intensity value at time t , BC is given by:

$$I(\mathbf{u}, t) = I(\mathbf{u} + \Delta\mathbf{u}, t + \Delta t), \quad (1)$$

where Δ denotes small shift in values. First-order approximation of Taylor series expansion of $I(\mathbf{u} + \Delta\mathbf{u}, t + \Delta t)$ gives:

$$\frac{\partial I}{\partial \mathbf{u}} \cdot \mathbf{v} = -\frac{\partial I}{\partial t}, \quad (2)$$

where $\mathbf{v} \doteq \frac{\Delta\mathbf{u}}{\Delta t}$ is the optical flow. Above constraint alone is not enough for flow estimation, hence additional constraints are usually imposed, e.g. spatial consistency. For a local event window $\Omega(\mathbf{u}, t)$, the optical flow can be estimated by solving the optimization problem:

$$\mathbf{v}^* = \arg \min_{\mathbf{v}} \sum_{\mathbf{u} \in \Omega} \left\| \nabla L(\mathbf{u}) \cdot \mathbf{v} + \frac{\partial L(\mathbf{u})}{\partial t} \right\|^2 \quad (3)$$

This can be solved in closed form using:

$$\mathbf{v}^* = -(\Phi^T \Phi)^{-1} \Phi^T \Theta, \quad (4)$$

where Φ and Θ are the matrices of spatial derivatives and temporal derivatives, respectively. This suggests that both spatial and temporal derivatives are essential, prompting the use of 4D correlation volumes in IR-based methods [10, 11, 20, 22]. They also utilize context events, which we argue is redundant in the following discussion.

3.1.2 Event Generation Model

Event cameras generate asynchronous events. Each event $e_k(t) \doteq (u_k, v_k, t, p_k)$ is a tuple that encodes space-time coordinates \mathbf{u}_k , t_k and the polarity $p_k \in \{-1, +1\}$ that represents the positive or negative change in the brightness. An event is generated when the change in log intensity $\Delta L(\mathbf{u}_k, t)$ reaches a certain threshold $\pm C$, i.e.

$$\Delta L(\mathbf{u}_k, t) = p_k C. \quad (5)$$

Where C is contrast threshold parameter and Δt is the time elapsed since the last event registered at \mathbf{u}_k . For sufficiently small Δt , it has been shown that $\Delta L \approx \nabla L \cdot \Delta \mathbf{u}$ [8], hence (5) can be rewritten as:

$$\frac{\partial L}{\partial \mathbf{u}} \cdot \mathbf{v} \Delta t = p_k C \quad (6)$$

Equations (2) and (6) suggest that events carry motion information.

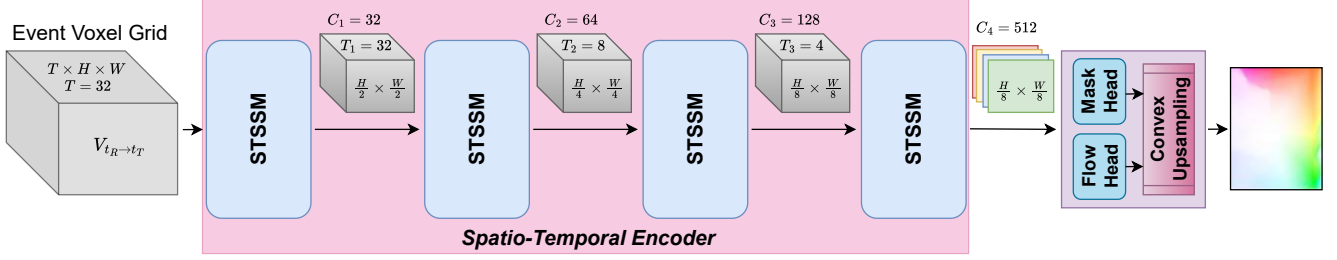


Figure 2. **Network Architecture** The Spatio-Temporal encoder utilizes successive STSSM Blocks to extract 2D ST feature-maps from input event volume $V_{t_R \rightarrow t_T}$. Then *Flow Head* and *Mask Head*, two-layered CNNs, are used to predict low-resolution flow and mask for convex upsampling to obtain full-scale flow prediction.

3.1.3 State Space Models

A linear time-invariant (LTI) system can be modeled by a set of first-order differential equations that can be represented in matrix form, called state-space representation. A system of N^{th} order can be represented by matrices, $\mathbf{A} \in \mathbb{R}^{N \times N}$, $\mathbf{B} \in \mathbb{R}^{N \times U}$, $\mathbf{C} \in \mathbb{R}^{M \times N}$ and $\mathbf{D} \in \mathbb{R}^{M \times U}$ as follows:

$$\frac{d\mathbf{x}}{dt} = \mathbf{A}\mathbf{x} + \mathbf{B}\mathbf{z}, \quad \mathbf{y} = \mathbf{C}\mathbf{x} + \mathbf{D}\mathbf{z}, \quad (7)$$

where $\mathbf{x}(t) \in \mathbb{R}^N$ is the state vector, while $\mathbf{z}(t) \in \mathbb{R}^U$ and $\mathbf{y}(t) \in \mathbb{R}^M$ are the inputs and outputs of the system, respectively. The matrix \mathbf{A} is most crucial in determining the dynamics of the system, while the matrices \mathbf{B} and \mathbf{C} define the input-to-state and state-to-output relations, respectively. Matrix \mathbf{D} is often not used as it establishes direct connection from input to output.

The continuous-time model in (7) can be *discretized* with a fixed step size Δ . For example, using zero-order-hold (ZOH) method, the discretized system can be obtained by $\bar{\mathbf{A}} = \exp(\Delta\mathbf{A})$ and $\bar{\mathbf{B}} = \mathbf{A}^{-1}(\exp(\Delta\mathbf{A}) - \mathbf{I})\mathbf{B}$ as follows:

$$\mathbf{x}_{k+1} = \bar{\mathbf{A}}\mathbf{x}_k + \bar{\mathbf{B}}\mathbf{z}_k, \quad \mathbf{y}_k = \mathbf{C}\mathbf{x}_k + \mathbf{D}\mathbf{z}_k. \quad (8)$$

Above formulation gives rise to a recurrent model that is also parallelizable. Moreover, usually a structure is imposed on matrix $\bar{\mathbf{A}}$ for computational efficiency. Thus, structured SSMs such as S4 [14] enjoy faster training compared to RNN and significantly better space and time complexity compared to Transformers.

Selective State Space Model (Mamba). Recently, a selection mechanism has been proposed for SSMs that makes the parameters Δ , $\bar{\mathbf{B}}$ and \mathbf{C} to be input dependent, making the system to be linear time-variant (LTV). This approach, dubbed as *Mamba* [12] is core part of our STSSM module for efficient processing of spatio-temporal event data. We also conduct ablation study to compare with other SSM variants such as S4 [14], S4D [13] and S5 [28].

As apparent from (3) that the optical flow estimation requires spatial context along with spatio-temporal correlations. IR-based approaches resort to utilizing two *successive-in-time* views from event data, reference view V_R and target view V_T [10, 11, 19]. We argue that given a sufficiently large spatio-temporal window, the events $\varepsilon(t_R, t_T) := \langle e(t) | t \in [t_R, t_T] \rangle$ are enough for flow estimation $F_{t_R \rightarrow t_T}$. We propose to use SSMs to extract spatio-temporal correlations along with spatial context only from $\varepsilon(t_R, t_T)$. We altogether avoid pyramids of 4D correlation volumes that have poor space and time complexity.

3.2. Network Details

First, we describe our network design, which is elemental for developing a highly efficient solution. Our network takes a volume of events as 3D space-time voxel grid. Then our carefully designed spatio-temporal encoder effectively extracts spatio-temporal information through a series of STSSM blocks. Finally, the prediction head takes these features to predict dense flow predictions at full resolution. Fig. 2 shows our network architecture with the necessary details.

3.2.1 Input Representation

We use voxel grid representation, similar to [10, 37]. For events in a temporal window $e_i \doteq (u_i, v_i, t_i, p_i) \in \varepsilon(t_R, t_T)$, the voxel grid $V_{t_R \rightarrow t_T} \in \mathbb{R}^{T \times H \times W}$ is encoded as:

$$V(\tilde{t}, u, v) = \sum_i p_i k_b(u - u_i) k_b(v - v_i) k_b(\tilde{t} - t_i^*) \quad (9)$$

where $\tilde{t} \in [0, T - 1]$ represents discretized temporal coordinate, and

$$t_i^* = (T - 1) \frac{t_i - t_R}{t_T - t_R}, \quad k_b(a) = \max(0, 1 - |a|).$$

In essence, the voxel grid encodes the spatio-temporal discretization error for each space-time coordinate in the event volume, along with the polarity.

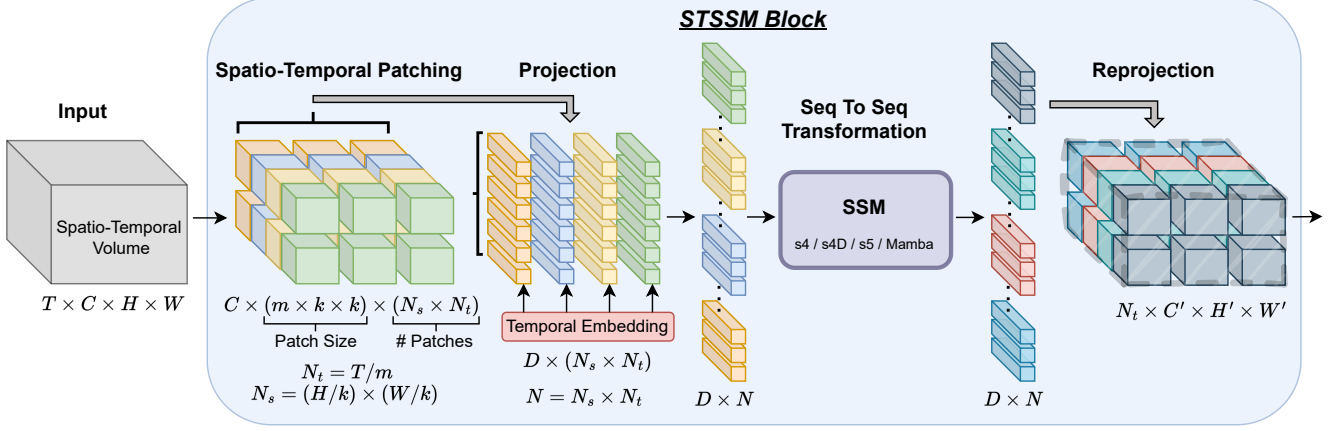


Figure 3. Structure of our STSSM Block. It processes 4D spatio-temporal volumes to extract ST features, keeping the spatio-temporal context intact, while reducing spatial and temporal dimensions to allow rich features with more number of channels.

3.2.2 Spatio-Temporal Encoder

Our spatio-temporal encoder $\mathcal{F}_\theta : \mathbb{R}^{T \times H \times W} \mapsto \mathbb{R}^{C \times \frac{H}{8} \times \frac{W}{8}}$ is consisted of four sequential STSSM blocks. The encoder takes in the spatio-temporal event volume $V_{t_R \rightarrow t_T}$ and encodes the spatio-temporal features into 2D feature maps with C channels.

Fig. 2 shows the inputs and outputs of each STSSM block. The output hyper volumes are progressively reduced in spatial and temporal dimensions to obtain more compact representations, while the channel dimension is increased to obtain rich feature-set. The patch dimensions in each successive STSSM block is spatially reduced and temporally increased, with $k = \{32, 8, 4, 1\}$ and $m = \{1, 4, 2, 4\}$, respectively. This is crucial to obtain fine-grained spatial features with more temporal context. The final STSSM block keeps the spatial dimension of the output to be the same as input, but reduce the temporal dimension to 1, resulting in 2D feature maps.

3.2.3 Prediction Head

Traditionally, a decoder network with skip connections is used to upscale the compact encoded features into full-scale predictions. However, they are computationally very heavy. For example, EV-Flownet [36] decoder has 80% share in total computational overhead of the network. Instead, we use convex upsampling as given in [30]. The Flow-head $\mathcal{H}_F : \mathbb{R}^{C \times \frac{H}{8} \times \frac{W}{8}} \mapsto \mathbb{R}^{2 \times \frac{H}{8} \times \frac{W}{8}}$ provides the flow estimate at 1/8 resolution. The Mask-head $\mathcal{H}_M : \mathbb{R}^{C \times \frac{H}{8} \times \frac{W}{8}} \mapsto \mathbb{R}^{576 \times \frac{H}{8} \times \frac{W}{8}}$ provides $(9 \times 8 \times 8)$ masks to create 8×8 patches using weighted average from 3×3 neighborhoods of low resolution flow.

3.3. STSSM Block

In this section we explain the spatio-temporal SSM (STSSM) block, which is the core novelty of this work. This block is specifically designed to deal with spatio-temporal volumes. Unlike 4D correlation volumes used in SOTA IR-based approaches [10, 11, 20, 30] to obtain spatio-temporal (ST) correlations from 2 views, we use a single ST volume and capture the ST correlations within the ST volume by using SSMs with a carefully designed spatio-temporal patching, projection and reprojection schemes. Fig. 3 summarizes the working of our STSSM block.

3.3.1 Spatio-Temporal Patching

Unlike video data, where each frame is a snapshot in time, the ST event volume (voxel grid) is sparse for slow motion and dense for fast motion. Hence, a single temporal bin does not necessarily contain all the spatial context. Therefore, to address this we introduce the idea of spatio-temporal patching. For an input of $\mathcal{I} \in \mathbb{R}^{C \times T \times H \times W}$, we create 3D patches of size $(m \times k \times k)$ for each of C channels, where m is the temporal dimension of the patch. The temporal dimension of output volume is given by $N_t = T/m$, with T being the input temporal dimension.

3.3.2 Projection

Similar to ViT, the purpose of projection is to obtain 1D features from the ST patches. This is done via a linear layer $\mathcal{L}_\theta : \mathbb{R}^{C \times P \times N} \mapsto \mathbb{R}^{D \times N}$, where P is the patch size and $N \doteq N_s \times N_t$ is the number of patches, with N_s, N_t being the number of patches in spatial and temporal dimensions, respectively.

3.3.3 Temporal Embedding

Considering SSMs to be LTI systems that map an input sequence to an output sequence through recurrence, as described in (8), the input signal should be in the same domain. However, our input consists of interleaved spatial and temporal domains. We untangle the spatial and temporal domains by introducing temporal embeddings, as illustrated in Fig. 3. Specifically, learnable parameters $\tau_\theta \in \mathbb{R}^{N_t \times D}$ are incorporated along the temporal dimension of the projected ST patches. This approach is analogous to the position encoding used in ViT. Our ablation study shows that position encoding is not needed and introduces unnecessary complication.

3.4. Seq-to-Seq Transformation

Recently, Mamba architecture has shown exceptional performance for sequence modeling across various modalities, such as language, audio, video and genomics [12]. Mamba boasts linear scaling in sequence length, making them far more efficient than transformers or other methods. Inspired by this breakthrough, we aim to leverage Mamba for capturing spatio-temporal correlations for high efficiency compared to existing methods that rely on 4D correlation volumes. We also conduct a study to compare Mamba with other SSM variants as well as transformers in similar settings in Sec. 4.4.

3.5. Reprojection

The output sequence from SSMs is reprojected to obtain a spatio-temporal volume from the input sequence data. each vector of size $D \times 1$ in the input sequence is reprojected to a 2D non-overlapping patch using C' kernels of size $(D \times l \times l)$, where l defines the spatial upscaling factor, while the temporal dimension remains the same. Hence, the reprojection module $\mathcal{R}_\theta : \mathbb{R}^{D \times (N_s \cdot N_t)} \mapsto \mathbb{R}^{N_t \times C' \times H' \times W'}$ transforms the sequence back to spatio-temporal volume. Note that $H' = (H \cdot l)/k$ and $W' = (W \cdot l)/k$, therefore, spatial scaling of the output is determined by the parameters l and k .

4. Experiments

4.1. Implementation Details

We used Mamba [12] PyTorch implementation for all of our STSSM modules in the network. In particular, 2 Mamba blocks were used in series with residual connections. The effectiveness of having multiple blocks in series is studied in ablations (Sec. 4.4).

Dataset. We used DSEC optical flow dataset [9] in this work. It comprises of driving sequences in both day and night times. Ground truth for test data is not available, so we created a validation split following [2] for training and

ablation studies. we apply random vertical and horizontal flipping and random time-scaling for data augmentations.

Training Details. Our network is implemented using Pytorch, trained using RTX 4090 GPUs with a batch size of 10. AdamW is used as the optimizer with a learning rate of 2×10^{-4} and a decay rate of 1×10^{-5} for 100 epochs. Additionally, the OneCycle LR scheduler is used for better convergence. Similar to previous works, we used L1 loss for all our networks.

$$\mathcal{L} = \frac{1}{|\mathcal{V}|} \sum_{(x,y) \in \mathcal{V}} \|F_j^{gt}(x,y) - F_j^{pred}(x,y)\|_1 \quad (10)$$

where, \mathcal{V} is the set of pixels with a valid ground truth flow.

	Type	Performance				GMAC
		EPE	AE	IPE	3PE	
MultiCM [27]	Optim.	3.47	13.98	76.6	30.9	-
TamingCM [24]	U-Net	2.33	10.56	68.3	17.8	-
OF_EV_SNN [2]	U-Net	1.71	6.338	53.7	10.3	168
EV-FlowNet [10, 36]	U-Net	2.32	7.90	55.4	18.6	62
E-RAFT [10]	IR	0.79	2.85	12.7	2.7	256
E-RAFT w/o WS [10]	IR	0.82	-	13.5	3.0	-
Bezier [11]	IR	0.75	2.68	11.9	2.4	-
TMA [20]	IR	0.74	2.68	10.9	2.7	522
ID-Net [34]	IR	0.77	3.00	12.1	2.0	222
Ours	SSM	1.11	4.29	26.4	5.0	32

Table 1. Evaluation results on DSEC [9] dataset.

	iters	EPE	AE	3PE	GMAC	Memory
ERAFT [10]	1	1.71	4.74	10.87	92.2	1.61 GB
	2	1.18	3.68	5.98	107.1	1.74 GB
TMA [20]	1	2.65	10.43	17.09	158.2	3.40 GB
	2	0.81	2.88	2.87	233.6	4.32 GB
Ours	1	1.11	4.23	5.00	32.4	1.2 GB

Table 2. Comparison with high-performance iterative methods with reduced number of iterations for fair comparison with comparable GMACs.

4.2. Benchmark Comparisons

In this section, we provide a comparison with SOTA approaches for event-based optical flow. Table 1 summarizes the comparison results. We divide the existing SOTA methods according to the type of network they employ. Optimization-based approaches usually perform inferior to learning-based approaches (also can be checked from the DSEC website). This can be explained due to the explicit assumptions on which the optimization frameworks rely.

Our method achieves an EPE of 1.11 pixels with a significantly lower computation cost (32 GMACs) compared to others. Compared to supervised EV-FlowNet [10, 36], our method offers 264% reduction in EPE with $2\times$ increase in computational efficiency. Compared to state-of-the-art E-RAFT [10] and TMA [20], our method offers $8\times$ and $16\times$ reductions in computational cost with only 0.32 px and 0.37 px increase in error (EPE), respectively.

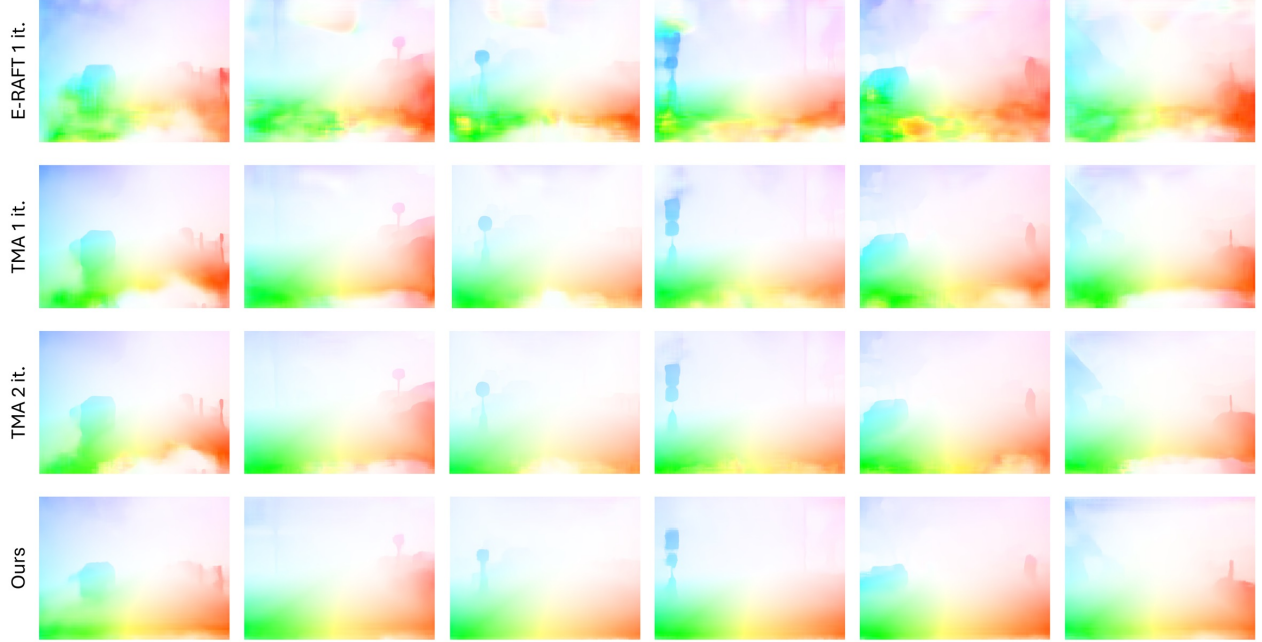


Figure 4. Optical flow prediction of our model on the DSEC dataset compared ground truth compared to state-of-the-art ERAFT [10] and TMA [20] methods. For fair comparison, their 1 iteration versions were used to generate the results. As ground truth is not available for test set, we also show the results using TMA (2 iters) for reference as it is closer to ground truth.

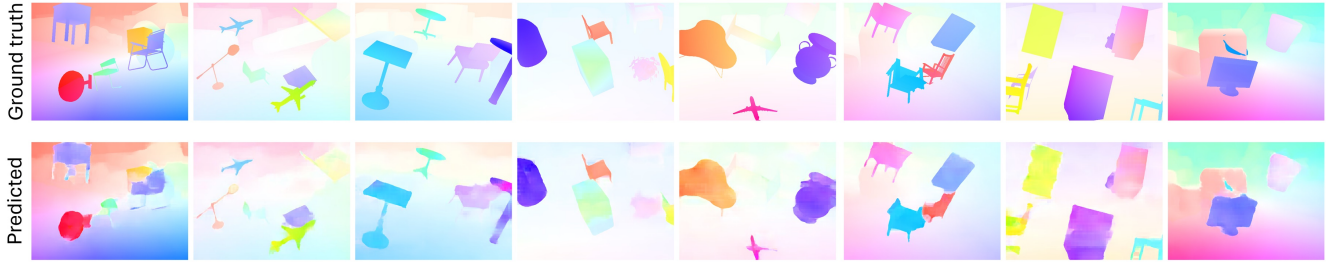


Figure 5. Optical flow prediction of our model on the BlinkFlow dataset compared ground truth. We demonstrate our model’s performance on cases with multiple objects, various directions, and occlusions.

Since IR-based methods [10, 20, 34] perform significantly better (See Table 1) at a cost of higher GMACs, we reduced the number of iterations to achieve a fair comparison in Table 2. Our method achieves significantly lower GMACs and demonstrates a clear performance advantage over state-of-the-art.

4.3. Qualitative Results

Fig. 4 shows the prediction results on the DSEC test set. Since ground truth is not available, we provide results using TMA [20] (with 2 iterations) for reference as it features low testing error (see Table 2). Compared to state-of-the-art ERAFT[10] and [20] (with 1 iteration), our method produces sharper and smoother predictions, even in the presence of high variations in flow magnitude, demonstrating the effectiveness of our STSSM module for spatio-temporal correlations.

Since DSEC does not contain many independently moving object (IMOs) and the motion is fairly coherent, we train and test our method on the synthetic BlinkFlow [19] dataset. We randomly split the data into 80% for training and 20% for testing. Fig. 5 shows the qualitative results obtained from the testing split, demonstrating the effectiveness of our method in dealing with IMOs; however, we find that it struggles in dealing with occlusion cases and thin objects, but otherwise it provides moderately sharp motion boundaries, even in complex and cluttered scenarios.

4.4. Ablation Studies

This section provides ablation studies to analyze the effect of our proposed design choices. Since the ground truth for DSEC is not available, we used the split of [2] for ablations, so there may be a discrepancy with the benchmarking results reported in Table 1.

Enc.	Mamba			Vi-T		
	EPE	3PE	Params	EPE	3PE	Params
No	0.90	2.7	8.68M	1.36	7.6	14.1M
t	0.88	2.6	8.68M	1.34	7.5	14.1M
t+p	0.89	2.6	11.53M	1.15	4.8	16.9M

Table 3. Ablation studies results for incorporating no encoding (No), temporal encoding (t), or both temporal and position encoding (t+p).

4.4.1 Temporal Encoding and Position Encoding

Position encoding is an elemental part of ViT [6] and has also been used with visual Mamba architectures [18, 21, 38]. However, we argue in Sec. 3.3 that our STSSM block uses SSM to extract spatio-temporal correlations, hence we only need temporal encoding to separate spatial and temporal domains. The results presented in Table 3 summarize our findings and supports our hypothesis.

	$\times N$	EPE	IPE	3PE	GMAC	Time
S4 [14]	1	1.1	38.1	4.2	28.2	20.9 ms
S4D [13]	1	1.07	36.4	4.0	28.2	10.8 ms
	2	1.3	47	6.5	31.4	16.8 ms
S5 [28]	1	1.14	40	4.6	29.8	7.1 ms
	2	0.96	31	3.0	34.7	12 ms
Mamba [12]	1	0.95	30	3.2	28.7	6.3 ms
	2	0.88	26.6	2.6	32.4	7.7 ms

Table 4. Ablation studies for different SSM variants with N blocks in series within each STSSM module.

4.4.2 SSM variants

Table 4 shows the results for different SSM variants. $N \in \{1, 2\}$ blocks in series were used for comparisons. The continuous-time model (S4) [14] has the worst execution speed, but offers similar performance to the diagonal version (S4D) [13]. However, S4D performance drops when multiple blocks are used in series. In contrast, the S5 [28] and Mamba [12] architectures provide better performance when multiple blocks are used in series. We suspect that this is due to the mixing layer present in the S4D architecture, implemented by position-wise linear layer. As expected, Mamba provides the best performance among all SSM variants with high computational efficiency and fast inference speed.

4.4.3 CNN vs Mamba vs Transformer

Our STSSM module is specifically designed to exploit SSMs to extract spatio-temporal correlations from spatio-temporal input data. In fact, 2D or 3D CNNs can also be used for the same purpose. We obtain results using different backbones (encoders) to specifically study the effectiveness of Mamba in STSSM. Conv (Baseline) refers to the

	N	EPE	IPE	3PE	Params	GMAC
Conv (Baseline)	-	1.08	31.6	3.3	3.7M	40.1
Conv 3D	-	0.91	26.4	3.2	9.1M	292.8
Vi-T	1	1.20	42.0	5.3	12.1M	50.3
	2	1.15	40.0	4.8	16.9M	75.7
Mamba	1	0.95	30.0	3.2	6.5M	28.7
	2	0.88	26.6	2.6	8.7M	32.4
Mamba + Vi-T	2	0.96	30.7	3.0	14.1M	57.0

Table 5. Comparison of Mamba and Transformer for seq-to-seq transformation in our STSSM module. (Mamba + Vi-T) refers to the network with the last STSSM block of the network uses Transformer and the rest use Mamba. N is the number of Mamba/Vi-T modules per STSSM block.

encoder from ERAFT [10], We also developed a 3D-CNN based encoder (referred to as Conv 3D), though more effective compared to the Baseline, it results in an exponential increase in computational cost (See Table 5). This explains how Mamba is extremely efficient for such task, given its linear scaling of complexity. We also replace Mamba with the transformer encoder [32] with 2 heads (referred to as Vi-T). However, transformer introduces unnecessary complexity, making it prone to overfitting and harder to train. In fact, the training curves obtained show noticeable noise, validating our hypothesis.

5. Conclusion

In this work, we introduce the powerful Mamba SSM for the first time for event-based optical flow. Our findings suggest that Mamba, and in general SSMs can be a good fit for processing spatio-temporal data such as event data. We developed a novel STSSM module that efficiently and effectively captures ST correlations and can also be cascaded to get compact representation with rich feature-set. We incorporate this module into our novel state-of-the-art network architecture designed for dense optical flow predictions from event volumes (space-time voxel grids). This results in the most efficient network to date that provides performance comparable to that of SOTA methods. Our findings reveal that Mamba is more suitable compared to transformers for extracting spatio-temporal correlations. They perform similarly to 3D CNNs but with exceptionally high computational efficiency for this particular task.

Acknowledgements

This work is supported by Sandoog Al Watan under Grant SWARD-S22-015, STRATA Manufacturing PJSC, and Advanced Research and Innovation Center (ARIC), which is jointly funded by Aerospace Holding Company LLC, a wholly-owned subsidiary of Mubadala Investment Company PJSC and Khalifa University for Science and Technology.

References

- [1] Thomas Bohnstingl, Ayush Garg, Stanisław Woźniak, George Saon, Evangelos Eleftheriou, and Angeliki Pantazi. Speech recognition using biologically-inspired neural networks. In *ICASSP 2022 - 2022 IEEE International Conference on Acoustics, Speech and Signal Processing (ICASSP)*, pages 6992–6996, 2022. 3
- [2] Javier Cuadrado, Ulysse Rançon, Benoit R Cottureau, Francisco Barranco, and Timothée Masquelier. Optical flow estimation from event-based cameras and spiking neural networks. *Frontiers in Neuroscience*, 17:1160034, 2023. 2, 3, 6, 7
- [3] Thomas Dalgaty, Thomas Mesquida, Damien Joubert, Amos Sironi, Pascal Vivet, and Christoph Posch. Hugnet: Hemispherical update graph neural network applied to low-latency event-based optical flow. In *Proceedings of the IEEE/CVF Conference on Computer Vision and Pattern Recognition*, pages 3952–3961, 2023. 2, 3
- [4] Ziluo Ding, Rui Zhao, Jiyuan Zhang, Tianxiao Gao, Ruiqin Xiong, Zhaoqi Yu, and Tiejun Huang. Spatio-temporal recurrent networks for event-based optical flow estimation. In *Proceedings of the AAAI conference on artificial intelligence*, pages 525–533, 2022. 2
- [5] Alexey Dosovitskiy, Philipp Fischer, Eddy Ilg, Philip Häusser, Caner Hazirbas, Vladimir Golkov, Patrick van der Smagt, Daniel Cremers, and Thomas Brox. FlowNet: Learning optical flow with convolutional networks. In *2015 IEEE International Conference on Computer Vision (ICCV)*, pages 2758–2766, 2015. 2
- [6] Alexey Dosovitskiy, Lucas Beyer, Alexander Kolesnikov, Dirk Weissenborn, Xiaohua Zhai, Thomas Unterthiner, Mostafa Dehghani, Matthias Minderer, Georg Heigold, Sylvain Gelly, Jakob Uszkoreit, and Neil Houlsby. An image is worth 16x16 words: Transformers for image recognition at scale. In *9th International Conference on Learning Representations, ICLR*, 2021. 8
- [7] Guillermo Gallego, Henri Rebecq, and Davide Scaramuzza. A unifying contrast maximization framework for event cameras, with applications to motion, depth, and optical flow estimation. In *2018 IEEE/CVF Conference on Computer Vision and Pattern Recognition*, pages 3867–3876, 2018. 2
- [8] Guillermo Gallego, Tobi Delbrück, Garrick Orchard, Chiara Bartolozzi, Brian Taba, Andrea Censi, Stefan Leutenegger, Andrew J Davison, Jörg Conradt, Kostas Daniilidis, et al. Event-based vision: A survey. *IEEE transactions on pattern analysis and machine intelligence*, 44(1):154–180, 2020. 3
- [9] Mathias Gehrig, Willem Aarents, Daniel Gehrig, and Davide Scaramuzza. Dsec: A stereo event camera dataset for driving scenarios. *IEEE Robotics and Automation Letters*, 6(3): 4947–4954, 2021. 1, 2, 6
- [10] Mathias Gehrig, Mario Millhäusler, Daniel Gehrig, and Davide Scaramuzza. E-raft: Dense optical flow from event cameras. In *2021 International Conference on 3D Vision (3DV)*, pages 197–206, 2021. 1, 2, 3, 4, 5, 6, 7, 8
- [11] Mathias Gehrig, Manasi Muglikar, and Davide Scaramuzza. Dense continuous-time optical flow from event cameras. *IEEE Transactions on Pattern Analysis and Machine Intelligence*, 2024. 2, 3, 4, 5, 6
- [12] Albert Gu and Tri Dao. Mamba: Linear-time sequence modeling with selective state spaces. *arXiv preprint arXiv:2312.00752*, 2023. 2, 3, 4, 6, 8
- [13] Albert Gu, Karan Goel, Ankit Gupta, and Christopher Ré. On the parameterization and initialization of diagonal state space models. *Advances in Neural Information Processing Systems*, 35:35971–35983, 2022. 2, 4, 8
- [14] Albert Gu, Karan Goel, and Christopher Ré. Efficiently modeling long sequences with structured state spaces. In *The International Conference on Learning Representations (ICLR)*, 2022. 2, 3, 4, 8
- [15] Jesse Hagenaars, Federico Paredes-Vallés, and Guido De Croon. Self-supervised learning of event-based optical flow with spiking neural networks. *Advances in Neural Information Processing Systems (NeurIPS)*, 34:7167–7179, 2021. 2, 3
- [16] Adarsh Kumar Kosta and Kaushik Roy. Adaptive-spikenet: event-based optical flow estimation using spiking neural networks with learnable neuronal dynamics. In *2023 IEEE International Conference on Robotics and Automation (ICRA)*, pages 6021–6027. IEEE, 2023.
- [17] Chankyu Lee, Adarsh Kumar Kosta, Alex Zihao Zhu, Kenneth Chaney, Kostas Daniilidis, and Kaushik Roy. SpikeFlowNet: event-based optical flow estimation with energy-efficient hybrid neural networks. In *European Conference on Computer Vision*, pages 366–382. Springer, 2020. 2, 3
- [18] Kunchang Li, Xinhao Li, Yi Wang, Yanan He, Yali Wang, Limin Wang, and Yu Qiao. Videomamba: State space model for efficient video understanding, 2024. 3, 8
- [19] Yijin Li, Zhaoyang Huang, Shuo Chen, Xiaoyu Shi, Hongsheng Li, Hujun Bao, Zhaopeng Cui, and Guofeng Zhang. Blinkflow: A dataset to push the limits of event-based optical flow estimation. *ArXiv*, abs/2303.07716, 2023. 2, 3, 4, 7
- [20] Haotian Liu, Guang Chen, Sanqing Qu, Yanping Zhang, Zhi-jun Li, Alois Knoll, and Changjun Jiang. Tma: Temporal motion aggregation for event-based optical flow. *arXiv preprint arXiv:2303.11629*, 2023. 1, 2, 3, 5, 6, 7
- [21] Yue Liu, Yunjie Tian, Yuzhong Zhao, Hongtian Yu, Lingxi Xie, Yaowei Wang, Qixiang Ye, and Yunfan Liu. Vmamba: Visual state space model. *arXiv preprint arXiv:2401.10166*, 2024. 3, 8
- [22] Xinglong Luo, Ao Luo, Zhengning Wang, Chunyu Lin, Bing Zeng, and Shuaicheng Liu. Efficient meshflow and optical flow estimation from event cameras. In *Proceedings of the IEEE/CVF Conference on Computer Vision and Pattern Recognition*, pages 19198–19207, 2024. 2, 3
- [23] Federico Paredes-Vallés and Guido CHE De Croon. Back to event basics: Self-supervised learning of image reconstruction for event cameras via photometric constancy. In *Proceedings of the IEEE/CVF Conference on Computer Vision and Pattern Recognition*, pages 3446–3455, 2021. 2
- [24] F. Paredes-Vallés, Kirk Y. W. Scheper, Christophe de Wagter, and G.C.H.E. de Croon. Taming contrast maximization for learning sequential, low-latency, event-based optical flow. *ArXiv*, abs/2303.05214, 2023. 2, 3, 6

- [25] Yannick Schnider, Stanisław Woźniak, Mathias Gehrig, Jules Lecomte, Axel von Arnim, Luca Benini, Davide Scaramuzza, and Angeliki Pantazi. Neuromorphic optical flow and real-time implementation with event cameras. In *2023 IEEE/CVF Conference on Computer Vision and Pattern Recognition Workshops (CVPRW)*, pages 4129–4138, 2023. [2](#)
- [26] Mark Schöne, Neeraj Mohan Sushma, Jingyue Zhuge, Christian Mayr, Anand Subramoney, and David Kappel. Scalable event-by-event processing of neuromorphic sensory signals with deep state-space models. *arXiv preprint arXiv:2404.18508*, 2024. [3](#)
- [27] Shintaro Shiba, Yoshimitsu Aoki, and Guillermo Gallego. Secrets of event-based optical flow. In *European Conference on Computer Vision (ECCV)*, pages 628–645, 2022. [2](#), [6](#)
- [28] Jimmy T.H. Smith, Andrew Warrington, and Scott Linderman. Simplified state space layers for sequence modeling. In *The International Conference on Learning Representations (ICLR)*, 2023. [2](#), [3](#), [4](#), [8](#)
- [29] Timo Stoffregen and Lindsay Kleeman. Simultaneous optical flow and segmentation (sofas) using dynamic vision sensor. *ArXiv*, abs/1805.12326, 2018. [2](#)
- [30] Zachary Teed and Jia Deng. Raft: Recurrent all-pairs field transforms for optical flow. In *Computer Vision–ECCV 2020: 16th European Conference, Glasgow, UK, August 23–28, 2020, Proceedings, Part II 16*, pages 402–419. Springer, 2020. [2](#), [3](#), [5](#)
- [31] Yi Tian and Juan Andrade-Cetto. Sdformerflow: Spatiotemporal swin spikeformer for event-based optical flow estimation, 2024. [2](#)
- [32] Ashish Vaswani, Noam Shazeer, Niki Parmar, Jakob Uszkoreit, Llion Jones, Aidan N Gomez, Łukasz Kaiser, and Illia Polosukhin. Attention is all you need. In *Advances in Neural Information Processing Systems*. Curran Associates, Inc., 2017. [8](#)
- [33] Zhexiong Wan, Yuchao Dai, and Yuxin Mao. Learning dense and continuous optical flow from an event camera. *IEEE Transactions on Image Processing*, 31:7237–7251, 2022. [3](#)
- [34] Yilun Wu, Federico Paredes-Vallés, and Guido CHE de Croon. Lightweight event-based optical flow estimation via iterative deblurring. *arXiv preprint arXiv:2211.13726*, 2022. [2](#), [6](#), [7](#)
- [35] Fan Yang, Li Su, Jinxiu Zhao, Xuena Chen, Xiangyu Wang, Na Jiang, and Quan Hu. Sa-flownet: Event-based self-attention optical flow estimation with spiking-analogue neural networks. *IET Computer Vision*, 2023. [2](#)
- [36] Alex Zihao Zhu, Liangzhe Yuan, Kenneth Chaney, and Kostas Daniilidis. Ev-flownet: Self-supervised optical flow estimation for event-based cameras. *arXiv preprint arXiv:1802.06898*, 2018. [2](#), [5](#), [6](#)
- [37] Alex Zihao Zhu, Liangzhe Yuan, Kenneth Chaney, and Kostas Daniilidis. Unsupervised event-based learning of optical flow, depth, and egomotion. In *Proceedings of the IEEE/CVF Conference on Computer Vision and Pattern Recognition*, pages 989–997, 2019. [2](#), [3](#), [4](#)
- [38] Lianghui Zhu, Bencheng Liao, Qian Zhang, Xinlong Wang, Wenyu Liu, and Xinggang Wang. Vision mamba: Efficient visual representation learning with bidirectional state space model. *ArXiv*, abs/2401.09417, 2024. [3](#), [8](#)
- [39] Nikola Zubic, Mathias Gehrig, and Davide Scaramuzza. State space models for event cameras. In *Proceedings of the IEEE/CVF Conference on Computer Vision and Pattern Recognition (CVPR)*, pages 5819–5828, 2024. [3](#)